THE JOURNAL OF PHYSICAL CHEMISTRY C

Article

pubs.acs.org/JPCC

Surface Diffusion of Hydrogen on Ni(100) from Ring Polymer Molecular Dynamics

Yury V. Suleimanov*,†

Physical and Theoretical Chemistry Laboratory, University of Oxford, South Parks Road, Oxford OX1 3QZ, U.K.

ABSTRACT: In this paper, we present a detailed ring polymer molecular dynamics (RPMD) study of the diffusion of hydrogen on Ni(100) using the well-established embedded atom method (EAM) interaction potential. We pay particular attention to the effects of lattice motion, transition state recrossing, and multiple hops. We show that all these effects can be assessed within a unified theoretical framework using RPMD. First, we study the low-temperature regime where the diffusion coefficient can be calculated by the random walk model. The crossover from thermally activated diffusion to almost temperature-independent quantum diffusion is found at around 70 K, in agreement with earlier quantum instanton calculations. We show that the recrossings of the transition state dividing surface become significant only below the crossover temperature in our RPMD calculations. The lattice motion slightly increases the diffusion coefficient above and slightly decreases it below the crossover temperature. We also show that quantizing the motion of the metal atoms has a negligible effect, even at very low temperatures. These last two observations are at variance with previous theoretical results obtained using the same interaction potential. We argue that this is primarily due to the different lattice models employed in the various calculations. Second, we studied the high-temperature regime. The diffusion coefficients are computed using the Einstein and Green−Kubo relations. Comparison of these results with those generated by the random walk model allows us to examine the role of correlated dynamical events in the diffusion. We find a noticeable contribution of correlated rebound events in our Einstein and Green−Kubo calculations, leading to a decrease in the diffusion coefficient compared to the random walk estimate at temperatures above 300 K.

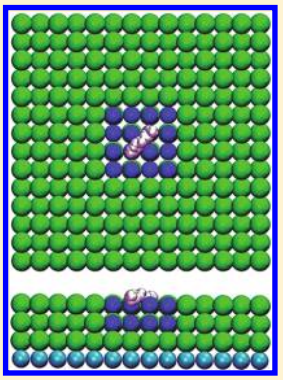

I. INTRODUCTION

The diffusion of adsorbed species plays a fundamental role in various surface processes such as heterogeneous catalysis, thermal desorption, and thin film growth.[1] Hydrogen diffusion on metal surfaces has been a particular focus of experimental and theoretical investigations due to its importance in heterogeneous catalysis. One of the most frequently studied systems is H on Ni(100). The hydrogen atom diffusion coefficient has been measured using laser-induced thermal desorption,[2,3] field emission microscopy,[4] and optical diffraction techniques.[5,6] These experiments have revealed a distinct transition from thermally activated diffusion at temperatures above 200 K to almost temperature-independent diffusion below 100 K. The low-temperature diffusion is presumably dominated by quantum mechanical tunnelling, although the measured diffusion coefficients and the crossover temperature have been reported to be very similar for hydrogen and deuterium,[4] which is difficult to explain in terms of a simple tunnelling mechanism.

These experimental findings have attracted a great deal of theoretical interest. A series of model interaction potentials have been constructed using the embedded atom method (EAM) to describe the interaction of hydrogen with the nickel surface.[7−14] Various forms of canonical variational transition state theory (CVT) with tunnelling corrections,[9,12,13] more elaborate quantum transition state theory (QTST) approaches including centroid density QTST[15−18] and the quantum instanton (QI) model,[19] the surrogate Hamiltonian method,[20−22] and a mixed quantum-classical approach[23−25] have all been used in conjunction with these EAM potentials to model hydrogen migration on Ni(100). However, the experimental observations have yet to be convincingly reproduced, and there are still many open issues concerning the mechanism of the diffusion.

It is well established that the diffusion is associated with the hopping of the adsorbed atom over transition states between adjacent surface lattice sites.[1] However, the results obtained using different dynamical methods have reached little concensus regarding three simple qualitative questions: How significant is transition state recrossing? How important are correlated multiple hops? Does lattice motion assist or hinder the diffusion? Some of the earlier theoretical results are even conflicting. For example, CVT, centroid density QTST, and QI calculations with the same EAM potential have predicted qualitatively different effects of the lattice motion on the H atom migration.[19] Unfortunately, rigorous quantum mechanical calculations of the adsorbate diffusion coefficient are unfeasible because of the many-body nature of the lattice motion. However, there are good reasons to believe that calculations using the recently developed ring polymer molecular dynamics (RPMD) model[26,27] may be able to shed some light on the problem.

The RPMD model is an approximate quantum mechanical simulation technique for condensed-phase systems, which is

Received: March 14, 2012
Revised: May 2, 2012
Published: May 7, 2012

   dx.doi.org/10.1021/jp302453z | J. Phys. Chem. C 2012, 116, 11141−11153

particularly well suited to the calculation of diffusion coefficients[28−33] and chemical reaction rates.[34−41] To give just one example that is relevant to the present study, RPMD simulations have recently explained a wide variety of experimental results concerning the diffusion of hydrogen, deuterium, and muonium atoms in liquid water and hexagonal ice over a temperature range spanning nearly 2 orders of magnitude.[32] Unlike mixed quantum-classical methods, RPMD treats all degrees of freedom on an equal footing, and unlike the CVT, QTST, and QI approaches, it includes a dynamical correction to transition state theory that accounts for recrossing of the transition state dividing surface.[40] In view of these features, it would seem that RPMD should provide an ideal tool for studying the diffusion of hydrogen atoms on metal surfaces.

In this paper, we present a comprehensive RPMD investigation of the diffusion of adsorbed hydrogen atoms on Ni(100), using a well-established EAM interaction potential that has often been used for this problem in the past.[11,12,19] We place particular emphasis on the effects of metal atom motion, transition state recrossing, and concerted hops, all of which can be assessed within a unified theoretical framework using RPMD. We begin in Section II by reviewing the basic equations of RPMD and describing how it can be used to study adsorbate diffusion in a computationally efficient manner at both high and low temperatures. In Section III we present the results of our simulations of the H + Ni(100) system and compare them with earlier experimental and theoretical studies, and in Section IV we present our conclusions.

II. GENERAL METHODOLOGY

IIA. Ring Polymer Molecular Dynamics. We shall confine our attention to low-coverage surface diffusion in which the interactions between the adsorbed atoms can be neglected. The relevant Hamiltonian is thus that of a single hydrogen atom interacting with a surface composed of $N - 1$ metal atoms. This can be written in the form

$$\hat{H} = \sum_{i=1}^{N} \frac{|\hat{\mathbf{p}}_i|^2}{2m_i} + V(\hat{\mathbf{r}}_1, ..., \hat{\mathbf{r}}_N) \tag{1}$$

where $\hat{\mathbf{p}}_i$ and $\hat{\mathbf{r}}_i$ are the momentum and position operators of the ith atom and m_i is its atomic mass. For convenience, we shall assume that the indices are ordered such that $i = 1$ labels the adsorbate and $i = 2, ..., N$ are the indices of the metal atoms.

The exact quantum mechanical diffusion coefficient of the adsorbed hydrogen atom is given by the Green−Kubo formula[42−44]

$$D(T) = \frac{1}{d}\int_0^\infty \tilde{c}_{\mathbf{v}\cdot\mathbf{v}}(t)\mathrm{d}t \tag{2}$$

where $d = 2$ is the dimensionality of the surface diffusion process, and $\tilde{c}_{\mathbf{v}\cdot\mathbf{v}}(t)$ is a Kubo-transformed adsorbate velocity autocorrelation function. The RPMD approximation to this is simply[28,30]

$$\tilde{c}_{\mathbf{v}\cdot\mathbf{v}}(t) = \frac{1}{(2\pi\hbar)^f Z_n}\int \mathrm{d}^f\mathbf{p}_0 \int \mathrm{d}^f\mathbf{r}_0 e^{-\beta_n H_n(\mathbf{p}_0,\mathbf{r}_0)}\bar{\mathbf{v}}_0\cdot\bar{\mathbf{v}}_t \tag{3}$$

where

$$Z_n = \frac{1}{(2\pi\hbar)^f}\int \mathrm{d}^f\mathbf{p}_0 \int \mathrm{d}^f\mathbf{r}_0 e^{-\beta_n H_n(\mathbf{p}_0,\mathbf{r}_0)} \tag{4}$$

is an n-bead path-integral approximation to the quantum mechanical partition function.[45,46] Here $f = 3Nn$ is the total number of ring polymer degrees of freedom; $\beta_n = \beta/n$ with $\beta = 1/(k_B T)$ is the appropriate reciprocal temperature; and $H_n(\mathbf{p},\mathbf{r})$ is the purely classical Hamiltonian of a system of harmonic ring polymers with an external potential of $V(\mathbf{r}_1, ..., \mathbf{r}_N)$ acting on each bead[26]

$$H_n(\mathbf{p}, \mathbf{r}) = H_n^0(\mathbf{p}, \mathbf{r}) + \sum_{j=1}^{n} V(\mathbf{r}_1^{(j)}, ..., \mathbf{r}_N^{(j)}) \tag{5}$$

where

$$H_n^0(\mathbf{p}, \mathbf{r}) = \sum_{i=1}^{N}\sum_{j=1}^{n}\left(\frac{|\mathbf{p}_i^{(j)}|^2}{2m_i} + \frac{1}{2}m_i\omega_n^2|\mathbf{r}_i^{(j)} - \mathbf{r}_i^{(j-1)}|^2\right) \tag{6}$$

with $\omega_n = 1/(\beta_n\hbar)$ and $\mathbf{r}_i^{(0)} \equiv \mathbf{r}_i^{(n)}$. In eq 3, $\bar{\mathbf{v}}_0$ and $\bar{\mathbf{v}}_t$ are the velocity vectors of the centroid of the H atom ring polymer at times 0 and t

$$\bar{\mathbf{v}}_t = \frac{1}{nm_1}\sum_{j=1}^{n}\mathbf{p}_1^{(j)}(t) \tag{7}$$

where the time-evolved momentum $\mathbf{p}_1^{(j)}(t)$ is obtained from the classical evolution under the ring polymer Hamiltonian $H_n(\mathbf{p},\mathbf{r})$ from the initial phase space point $(\mathbf{p}_0,\mathbf{r}_0)$.

Alternatively and equivalently, the diffusion coefficient can be obtained from the Einstein relation[43,44]

$$D(T) = \frac{1}{2d}\lim_{t\to\infty}\frac{\langle|\Delta\bar{\mathbf{r}}_t|^2\rangle}{t} \tag{8}$$

where $|\Delta\bar{\mathbf{r}}_t|^2$ is the mean squared displacement

$$|\Delta\bar{\mathbf{r}}_t|^2 = |\bar{\mathbf{r}}_1(t) - \bar{\mathbf{r}}_1(0)|^2 \tag{9}$$

of the hydrogen atom centroid

$$\bar{\mathbf{r}}_1(t) = \frac{1}{n}\sum_{j=1}^{n}\mathbf{r}_1^{(j)}(t) \tag{10}$$

and we have introduced the shorthand notation

$$\langle\cdots\rangle = \frac{\int \mathrm{d}^f\mathbf{p}_0\int \mathrm{d}^f\mathbf{r}_0 e^{-\beta_n H_n(\mathbf{p}_0,\mathbf{r}_0)}(\cdots)}{\int \mathrm{d}^f\mathbf{p}_0\int \mathrm{d}^f\mathbf{r}_0 e^{-\beta_n H_n(\mathbf{p}_0,\mathbf{r}_0)}} \tag{11}$$

for an average over the canonical ensemble. Note in passing that eqs 2 and 8 provide an entirely general way to calculate the H atom diffusion coefficient that is free from any assumptions about the diffusion mechanism.

IIB. Low-Temperature Simulations. At low temperatures, the average time between successive surface hops increases greatly, making direct molecular dynamics simulations using eqs 2 and 8 prohibitively expensive. This difficulty is usually overcome by employing a random walk model,[47] in which one assumes that the diffusion arises from of a sequence of uncorrelated hops between neighboring surface sites. Within this assumption, the mean square displacement can be expressed as

$$\langle|\Delta\bar{\mathbf{r}}_t|^2\rangle \approx \sigma k(T) b^2 t \tag{12}$$

where σ is the number of equivalent hopping directions; b is the jump length (the distance between two adjacent site centers); and $k(T)$ is the rate coefficient for site-to-site hopping. For hydrogen migration on Ni(100), the hopping path is from a

dx.doi.org/10.1021/jp302453z | J. Phys. Chem. C 2012, 116, 11141−11153

4-fold hollow site to a nearest-neighbor 4-fold hollow site via a 2-fold bridge site (see Figure 1), and so $\sigma = 4$. The diffusion coefficient is therefore

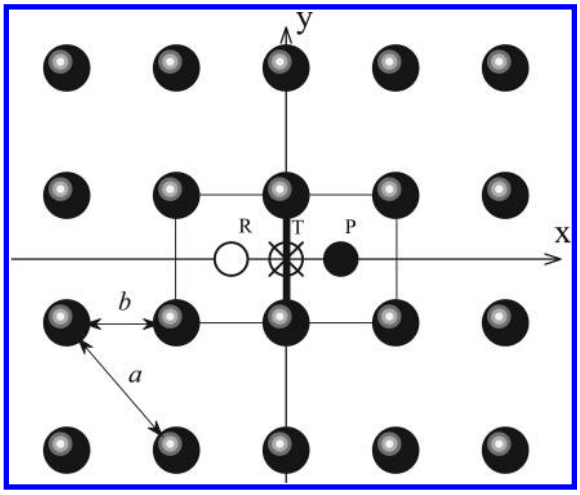

Figure 1. Schematic diagram of the (100) surface of a face-centered cubic (fcc) crystal. The square cells surrounded by solid lines are used to define the region of site-to-site hopping. The dividing surface between the two cells is shown as a thick line. T (transition state, 2-fold bridge site ⊗) shows the hydrogen atom at the saddle point on the potential energy surface between the two cells. R (reactant, 4-fold hollow site ○) at $(-b/2,0)$ and P (product, 4-fold hollow site ●) at $(+b/2,0)$ show the hydrogen atom equilibrium positions. a is the lattice constant of the bulk fcc lattice, and $b = a/\sqrt{2}$ is the hopping distance. These are 3.52 and 2.49 Å, respectively, in the case of the Ni(100) surface.

$$D(T) \approx k(T)b^2 \tag{13}$$

In the random walk model, the calculation of the diffusion coefficient is thus reduced to evaluate the rate coefficient for site-to-site hopping. Note that this approximation is only valid if the adsorbed H atom spends enough time thermalizing in each site to lose all memory of its previous hop, so that all directions for the next hop are equally likely.

The site-to-site hopping rate can be calculated by combining RPMD rate theory[34,35] with the Bennett−Chandler method.[48,49] This approach has been discussed extensively in our recent papers,[32,36,37,40] so only the final working expressions will be given here. The method begins by introducing a reaction coordinate $s(\mathbf{r})$ which monitors the progress from the reactant ($s < 0$) to the product ($s > 0$) site during a surface hop. For a H atom ring polymer on the Ni(100) surface, a suitable reaction coordinate is simply $s(\mathbf{r}) = \bar{x}_1$, where $\bar{x}_1$ is the x component of the H atom centroid and the y component is restricted to the range $-b/2 \le \bar{y}_1 \le +b/2$ (see Figure 1).

The RPMD rate coefficient is then calculated as a product of two factors[32,36,37,40]

$$k(T) = k^{\mathrm{QTST}}(T)\kappa(t_{\mathrm{p}}) \tag{14}$$

Here, the first factor, $k^{\mathrm{QTST}}(T)$, is the centroid density[50,51] QTST rate. This can be calculated from the potential of mean force along the reaction coordinate

$$W(s) = -\frac{1}{\beta}\ln\langle\delta[s - s(\mathbf{r})]\rangle \tag{15}$$

as[36]

$$k^{\mathrm{QTST}}(T) = \frac{1}{(2\pi\beta m_1)^{1/2}}\frac{e^{-\beta W(0)}}{\int_{-b}^{0} e^{-\beta W(s)}\mathrm{d}s} \tag{16}$$

where the integral in the denominator extends over the reactant site (see Figure 1).

The second factor in eq 14, $\kappa(t_{\mathrm{p}})$, is a time-dependent ring polymer transmission coefficient[32,36]

$$\kappa(t) = \frac{\langle\delta[s(\mathbf{r}_0)]\dot{s}(\mathbf{r}_0)h[s(\mathbf{r}_t)]\rangle}{\langle\delta[s(\mathbf{r}_0)]\dot{s}(\mathbf{r}_0)h[\dot{s}(\mathbf{r}_0)]\rangle} \tag{17}$$

evaluated at a time t_{p} in the "plateau" region[49] where the transient oscillations associated with the re-crossing of the transition state dividing surface have died away. The delta function $\delta[s(\mathbf{r}_0)]$ in the numerator of eq 17 confines initial configurations to the dividing surface $s(\mathbf{r}_0) = 0$; the velocity factor $\dot{s}(r_0)$ collects the flux through this dividing surface; and the step function $h[s(\mathbf{r}_t)]$ selects ring polymer trajectories that are on the product side of the surface at time t. The interpretation of the denominator is much the same, except that now $h[s(\mathbf{r}_t)]$ has been replaced by its short-time limit $h[\dot{s}(\mathbf{r}_0)]$, which normalizes the transmission coefficient such that $\kappa(t \to 0_+) = 1$. As we have discussed extensively in our recent papers, the inclusion of the transmission coefficient $\kappa(t_{\mathrm{p}})$ in eq 14 gives a rate coefficient $k(T)$ that is rigorously independent of the choice of the transition state dividing surface.[35] This is clearly an appealing aspect of the RPMD theory which insofar as we are aware is not shared by any other approximate quantum mechanical theory of reaction rates.[40]

III. APPLICATION TO HYDROGEN DIFFUSION ON NI(100)

IIIA. Computational Details. As our model for the interaction potential, we have chosen the embedded atom method (EAM).[7,8] This has been extensively used in the past to model surface and interior hydrogen migration in nickel.[8−16,19,20,22,52] The EAM is a semiempirical method based on density functional theory.[7,8] Several EAM parametrizations have been developed for hydrogen and nickel and shown to reproduce various experimental quantities. We have chosen to use parameter set 4 (EAM4) from ref 11, which is expected to provide a reasonable description of hydrogen on the (100) face of Ni. This potential has been used in several previous calculations of the hopping rate on Ni(100),[12,19] which gives us an opportunity to compare our RPMD results with those of earlier work. All of the information needed to implement the EAM4 potential can be found in refs 8, 10, and 11.

The structural model we have adopted for the diffusion of H on Ni(100) consists of a single hydrogen atom adsorbed on a four-layered slab of 392 Ni atoms, with 98 atoms in each layer. This number of Ni atoms was chosen so that the length of the simulation box in the two lateral directions was more than twice the cutoff distance of the EAM4 potential (10 Å).[11] Periodic boundary conditions were employed in the two dimensions parallel to the surface, and the bottom layer of the lattice was held fixed. Limited studies were also performed using a lattice with an additional fifth layer added to the bottom, and the computed rate coefficients were unchanged to within less than 1%. The results presented here with four layers are therefore converged with respect to the size of the lattice.

dx.doi.org/10.1021/jp302453z | J. Phys. Chem. C 2012, 116, 11141−11153

Three types of the nickel lattice were considered to study the effect of lattice motion and lattice quantisation:

- Rigid lattice - all 392 nickel atoms were held fixed at their equilibrium lattice positions;
- Classical lattice - the top 3 × 98 Ni atoms were treated classically, while the Ni atoms in the bottom layer were held fixed;
- Quantum lattice - the same as the classical lattice except that 16 atoms surrounding the reactant and product sites and lying directly beneath these sites were treated quantum mechanically; this is similar to the quantization scheme used in the previous QI calculations.[19]

The quantum lattice is shown in Figure 2.

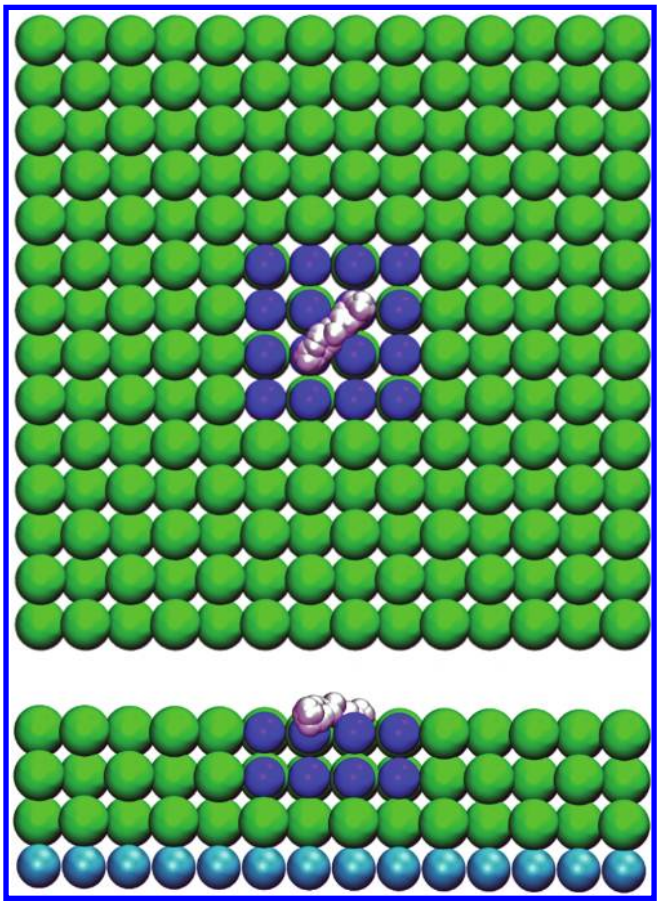

Figure 2. Plan and cross-sectional view of a model (quantum) lattice of Ni(100) used in RPMD studies of hydrogen surface diffusion. The white circles are H atom beads dispersed along the reaction path with the centroid of the ring polymer pinned to the transition state. The blue circles are Ni atoms that are treated quantum mechanically (as ring polymers), and the green circles are Ni atoms that are treated classically (as single bead particles). The cyan circles are the fixed Ni atoms in the bottom layer.

In our first set of calculations, the surface diffusion coefficients were estimated using the random walk model discussed in Section IIB. Calculations were performed for two isotopes of the adsorbed atom at temperatures ranging from 30 to 1000 K. For hydrogen, we considered all three types of lattice, although in the case of the quantum lattice only at representative temperatures of 40 and 300 K. For deuterium, we limited our calculations to the rigid lattice. The number of ring polymer beads required for convergence depended on the temperature and ranged from 24 at 1000 K to 64 at 30 K. The convergence was tested with up to 80 beads at the lowest temperature. For the rigid lattice, we also repeated all the calculations with the hydrogen atom ring polymer collapsed to a classical particle.

As in our previous RPMD studies,[32,37,40] the centroid density QTST rate constant was calculated using umbrella integration.[53−55] 120 biasing windows were evenly spaced in the interval -1.45 Å $\leq s \leq 0.15$ Å. The force constant of the harmonic biasing potential was varied from 5.44 meV a_0^{-2} at 30 K to 54.42 meV a_0^{-2} at 1000 K. For each umbrella window, 120 initial configurations were generated, and following an equilibration period of 15 ps, the force on the centroid of the ring polymer along the reaction coordinate was averaged over 25 ps trajectories in the presence of an Andersen thermostat.[56] The ring polymer equations of motion were integrated using a symplectic integrator involving alternating momentum updates and free ring polymer evolutions,[26] with a time step of 0.5 fs.

The transmission coefficient $\kappa(t)$ was calculated by running 50 recrossing trajectories for each of 200 independent configurations of the system at $t = 0$ with the centroid of the H atom constrained to the dividing surface using the RATTLE algorithm.[57] The recrossing trajectories were propagated in the absence of the thermostat and the dividing surface constraint until a plateau was observed in $\kappa(t)$. The plateau times t_p were found to be around 1 ps at $T = 30$ K, 0.5 ps for $40 \leq T \leq 60$ K, and 0.05 ps for $80 \leq T \leq 1000$ K, for both isotopes. The site-to-site RPMD hopping rate was calculated using eq 14 and the random walk diffusion coefficient using eq 13.

At high temperatures ($T \geq 300$ K), the constrained simulations on the dividing surface in the calculation of $\kappa(t)$ and the umbrella integration near the barrier region in the calculation of $k^{QTST}(T)$ were found to be long enough to include hopping to the neighboring bridge sites along the y axis (see Figure 1). Whenever such bridge-to-bridge jumps took place, the trajectories were simply restarted from random configurations taken from the previous simulation.

In a second set of calculations, the RPMD surface diffusion coefficients were obtained from the Green−Kubo and Einstein relations in Section IIA. Calculations were restricted to the temperature range $200 \leq T \leq 1000$ K because at lower temperatures the direct molecular dynamics simulations were unfeasible. Only one isotope (hydrogen) and two lattice types (rigid and classical) were considered, quantum effects in the Ni lattice motion having been found to be negligible in our random walk model calculations. At each temperature, 4000 RPMD trajectories were initiated by placing the H atom at positions slightly above the surface. The hydrogen was then allowed to land and thermalize under the influence of an Andersen thermostat for a period of 50 ps ($T \leq 400$ K), 5 ps ($500 \leq T \leq 700$ K, or 0.5 ps ($T \geq 800$ K). The configuration and velocities at the end of this period were used as initial conditions for a dynamics run with the thermostat switched off.

It is clear from eqs 2 and 8 that the simulation time t_{sim} should be long enough for $\tilde{c}_{v\cdot v}(t)$ to become zero and $\langle|\Delta\bar{\mathbf{r}}_t|^2\rangle/t$ to reach a constant within this time. In the present calculations, t_{sim} was extended further so that it was also long enough to include a sufficient number of hops (more than 1000 in total) to ensure good statistics for the analysis described in Section IIIC. This required simulations ranging from 5 ps at 1000 K to 500 ps at 200 K. In spite of these long simulation runs, no constraints were imposed to prevent thermal desorption, which

dx.doi.org/10.1021/jp302453z | J. Phys. Chem. C 2012, 116, 11141−11153

was not observed even at the highest temperature we considered.

IIIB. Low-Temperature Diffusion. In this section, we analyze the hydrogen diffusion on the Ni(100) surface in the temperature interval 30−300 K. In this regime, the hydrogen atom spends a significant amount of time at each lattice site before hopping,[9,12−19] and its diffusive motion is therefore expected to be well described by the random walk model.

Figure 3 presents the calculated centroid potentials of mean force along the reaction path for the site-to-site hopping at two

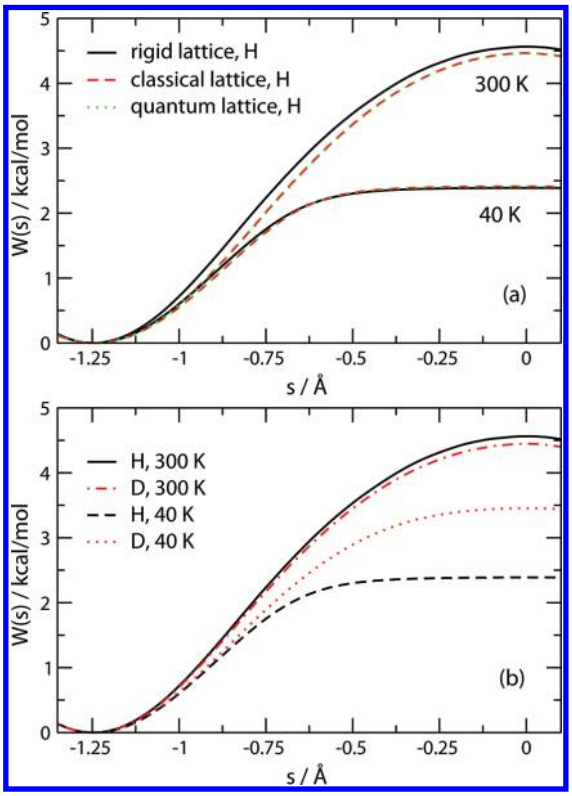

Figure 3. Centroid potentials of mean force along the reaction coordinate for site-to-site hopping at 40 and 300 K. The reactant (4-fold) site is located at $s = -1.245$ Å and the transition state (bridge) site at $s = 0$. (a) Results for hydrogen on the rigid, classical, and quantum Ni(100) lattices. The computed potentials of mean force for the classical and quantum lattices are the same to within graphical accuracy. (b) Comparison of results for hydrogen and deuterium on the rigid lattice.

representative temperatures, 40 and 300 K. Consider first the upper panel, which shows the results obtained for hydrogen with the three different treatments of the Ni lattice. Allowing for the classical motion of the Ni atoms is seen to decrease the free energy barrier to site-to-site hopping at 300 K and to increase it at 40 K. At both temperatures, the difference between the height of the rigid and dynamic barriers is less than a few percent. The effect of the lattice motion on the rate constant will however be larger than this owing to the exponential dependence on $W(s)$ in eq 16. A more striking observation is that quantizing the motion of the Ni atoms closest to the surface hydrogen has virtually no effect on the free energy barrier at either temperature: the results for the classical and quantum lattices are the same to within graphical accuracy. We believe this is because the (free) ring polymer radius of gyration of a Ni atom in the quantized calculation, $\langle r_G^2 \rangle^{1/2} = \hbar/(4mk_BT)^{1/2}$, is still very small (~7 pm) even at 40 K. Since the potential energy experienced by a Ni atom in the neighborhood of its equilibrium lattice site changes only very slightly over this length scale, there is hardly any difference between treating the atom as a ring polymer and shrinking the ring polymer to a classical particle.

Another interesting feature of the potential of mean force is its unusual isotope dependence. The lower panel of Figure 3 shows that at low temperatures the free energy barrier is much higher for deuterium than for hydrogen, but as the temperature increases, the barrier becomes higher for hydrogen. The inverse kinetic isotope effect at high temperatures is clearly due to a greater zero-point energy contribution to the free energy at the transition state than at the reactant minimum, and we have confirmed this by calculating the harmonic zero-point energies of the adsorbed atom at both positions. For hydrogen, the resulting zero-point energy corrected barrier height is 4.73 kcal/mol, whereas for deuterium it is 4.55 kcal/mol, in good qualitative agreement with the more accurate (anharmonic) free energy barriers obtained from the potentials of mean force in Figure 3 at 300 K. The more pronounced isotope effect at low temperatures is due to tunnelling, which leads to a significantly smaller free energy barrier for hydrogen than for deuterium. Note especially that the hydrogen free energy barrier becomes much broader and flatter at 40 K than it is at 300 K; this is a characteristic feature of the tunnelling regime.

Figure 4 presents the RPMD transmission coefficients $\kappa(t)$ computed at different temperatures for hydrogen diffusion

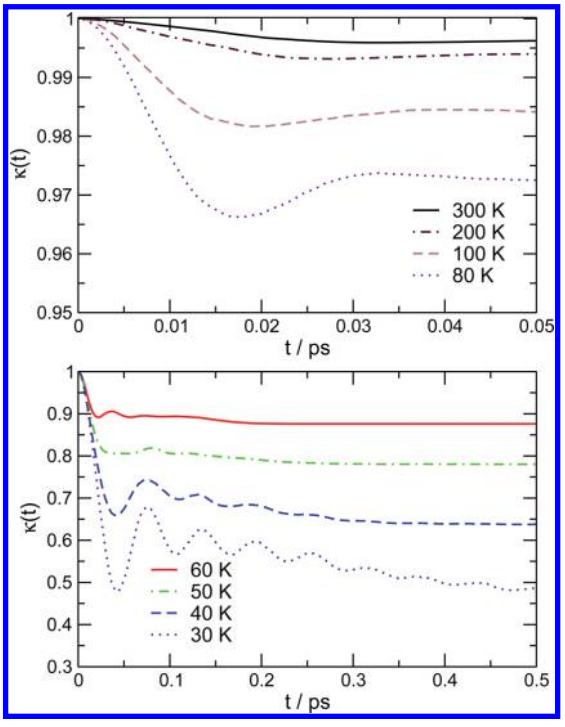

Figure 4. Time-dependent RPMD transmission coefficients for the site-to-site hopping of H on the Ni(100) surface at different temperatures. The results are for the rigid lattice.

on the rigid lattice. One sees that a significant fraction of the RPMD trajectories recrosses the transition state dividing surface at low temperatures. The plateau in the RPMD transmission coefficient decreases with decreasing temperature and is as small as 0.47 at 30 K. A similar temperature dependence of $\kappa(t)$ has

dx.doi.org/10.1021/jp302453z | J. Phys. Chem. C 2012, 116, 11141−11153

been seen in earlier RPMD studies of gas-phase reactions.[37,40] The increased recrossing at low temperatures originates from the functional form of the transition state dividing surface $s(\mathbf{r}) = 0$, which we have chosen here to be a function of the centroid of the hydrogen atom (see Section IIB). Richardson and Althorpe[58] have shown that the optimal reaction coordinate is in general a function of several normal modes of the ring polymer and that the centroid becomes a poor approximation at temperatures below the crossover temperature $T_c = \hbar\omega_b/2\pi k_B$, where $i\omega_b$ is the imaginary frequency at the transition state saddle point. For H diffusion on a rigid Ni(100) lattice, we find T_c for the EAM4 potential to be 67 K, which is precisely where the transmission coefficient in Figure 4 begins to decrease. At temperatures above 70 K, the plateau value of the transmission coefficient is close to unity.

Another consequence of using a reaction coordinate based on the ring polymer centroid is the appearance of short-time oscillations in the RPMD transmission coefficient at low temperatures, which are best seen at $T = 30$ K in Figure 4. Similar oscillations were found in a previous RPMD study of hydrogen diffusion in hexagonal ice at 8 K,[32] where they were attributed to the vibrational motions of the beads of the ring polymer in the reactant and product cavities as the centroid passed over the transition state. The oscillations do not have any physical significance since they would disappear if one were to use a more appropriate (instanton-based[58]) dividing surface involving the internal modes of the ring polymer; this would not have any effect on the final RPMD rate coefficient, which is rigorously independent of the choice of the reaction coordinate $s(\mathbf{r})$ and the dividing surface $s(\mathbf{r}) = 0$.[35]

From Figure 4, one also sees that the recrossing associated with a single site-to-site hopping event ceases rather quickly on the time scale of the lattice motion. When $T > 70$ K, $\kappa(t)$ reaches a plateau value within 50 fs, whereas the period of the lattice vibrations is at least 300 fs (the surface Debye temperature of the EAM4 potential is around 160 K). This suggests that the recrossing dynamics will not be affected significantly by the lattice motion, at least at high temperatures. Figure 5 shows that this is the case even at very low temperatures, where the transmission coefficient decays more slowly. The H atom RPMD transmission coefficients at $T = 40$ K nearly coincide for all three types of lattice (rigid, classical, and quantum). The same figure also shows that there is a significant isotope effect in the transmission coefficient at low temperatures, the plateau in the transmission coefficient for D being significantly higher than that for H. This is consistent with what we have said above about how the transmission coefficient begins to decrease below the crossover temperature, which is 67 K for hydrogen but only 48 K for deuterium.

Note that if one examines the behavior of $\kappa(t)$ on a very long time scale, up to times much greater than the average time between flights (the inverse of the reaction rate, $(k^{(n)}(T))^{-1}$), one may find that, after the plateau regime, it becomes an exponentially decaying function which ultimately tends to zero. This happens because the crossing dynamics at $t = 0$ is uncorrelated with the one in the long-time limit; i.e., the adatom recrosses the dividing surface $s(\bar{\mathbf{q}}_1(t))$ while performing "another" flight. This is most easy to observe as the temperature is increased so that $(k^{(n)}(T))^{-1}$ decreases. As an example, the lower panel of Figure 5 demonstrates the long-time behavior of the RPMD transmission coefficients computed at $T = 300$ K. From this figure, one may also notice that the RPMD transmission coefficients start to decay rather quickly after reaching the

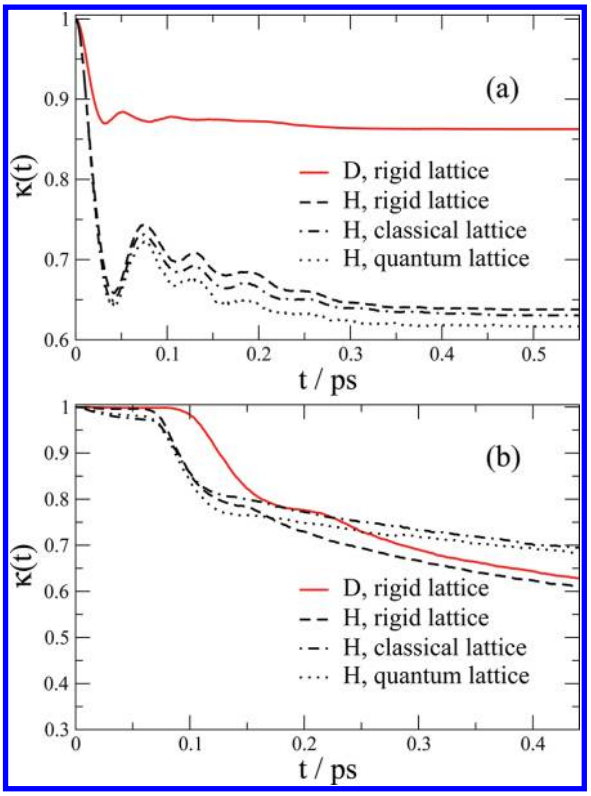

Figure 5. Time-dependent RPMD transmission coefficients for the site-to-site hopping of H and D on the Ni(100) surface. (a) Results for the rigid, classical, and quantum lattices at 40 K. (b) Long-time behavior of the transmission coefficients at 300 K.

plateau value at around $t_p = 0.05$ ps. This suggests that at such high temperatures the adatom may not have enough time to equilibrate thoroughly before performing the next hop. Therefore, the random walk model may become, strictly speaking, not applicable. Despite this fact, the small plateau region was found even at 1000 K, as t_p becomes roughly independent of temperature at $T \geq 80$ K and is around 0.05 ps. Therefore, formally, we were able to isolate the recrossing dynamics of the single site-to-site hopping event and obtain the RPMD rate coefficients for the entire temperature range considered here.

Table 1 summarizes all of the rate coefficients for site-to-site hopping we have computed in the temperature range from 30 to 300 K. We first note that the centroid density QTST and RPMD rate coefficients for H atom hopping become very weakly temperature dependent below around 70 K, indicating the crossover to the regime where tunnelling dominates the hopping process. For D atom hopping, the transition to a weakly temperature-dependent rate coefficient occurs at around 50 K because of the lower crossover temperature (48 K rather than 67 K according to the simple parabolic barrier estimate). As a result, a very large H/D kinetic isotope effect is observed below 70 K, owing to the greater tunnelling of the H atom. Above 200 K, the H/D kinetic isotope effect is much smaller, and in fact it is even smaller than the purely classical factor of $\sqrt{2}$ that comes from the mass dependence of the pre-exponential factor in eq 16; this is because of the inverse kinetic energy isotope effect in the free energy profiles for H and D at high temperatures seen in Figure 3.

Notice also that, for hydrogen, the centroid density QTST rate actually increases on going from 40 to 30 K. This unphysical

Table 1. Classical, Centroid Density QTST, and RPMD Rate Coefficients for Hydrogen and Deuterium Hopping from One Hollow to Another Adjoining a Hollow Site on the Ni(100) Surface in the Temperature Interval between 30 and 300 K[a]

		T (K)							
method	lattice	30	40	50	60	80	100	200	300
					Hydrogen Diffusion				
classical	rigid	1.30 (−17)	4.03 (−10)	1.23 (−5)	1.21 (−2)	6.67 (1)	1.17 (4)	3.56(8)	1.13 (10)
QTST	rigid	1.80 (0)	1.34 (0)	1.37 (0)	1.79 (0)	1.27 (2)	9.62 (3)	1.99 (8)	7.15 (9)
	classical	9.97 (−1)	9.55 (−1)	9.58 (−1)	1.67 (0)	1.25 (2)	9.84 (3)	2.15 (8)	7.67 (9)
	quantum		9.54 (−1)						7.77 (9)
RPMD	rigid	8.50 (−1)	8.56 (−1)	1.07 (0)	1.57 (0)	1.23 (2)	9.47 (3)	1.98 (8)	7.12 (9)
	classical	4.72 (−1)	6.02 (−1)	7.37 (−1)	1.45 (0)	1.19 (2)	9.50 (3)	2.10 (8)	7.48 (9)
	quantum		5.88 (−1)						7.60 (9)
					Deuterium Diffusion				
QTST	rigid	7.46 (−7)	1.39 (−6)	5.28 (−5)	1.20 (−2)	3.25 (1)	4.94 (3)	1.65 (8)	6.04 (9)
RPMD	rigid	5.25 (−7)	1.20 (−6)	5.06 (−5)	1.18 (−2)	3.22 (1)	4.91 (3)	1.64 (8)	6.02 (9)

[a]Rate coefficients are given in s^{-1}, and numbers in parentheses denote powers of ten.

behavior arises because the centroid of the hydrogen atom provides an increasingly poor reaction coordinate as the temperature is lowered, as evidenced by the RPMD transmission coefficients in Figure 4. This breakdown of the centroid density QTST approximation to the rate at low temperatures is well-known in the literature,[58−61] and a similar unphysical temperature dependence of the QTST rate has recently been seen in a study of the F + H_2 reaction in the gas phase.[37] By contrast, the RPMD calculation gives a rate that is independent of the choice of the reaction coordinate and decreases monotonically as the temperature is lowered.

Table 1 also shows that treating the hydrogen atom quantum mechanically is extremely important for proper determination of the rate coefficient. Below the crossover temperature, where the quantum tunnelling effect is dominant, the purely classical rate coefficients in the table are several orders of magnitude smaller than those obtained from centroid density QTST and RPMD. At higher temperatures, the zero-point energy effect starts to play a dominant role. This effect is also left out of the classical simulations. The classical barrier of 4.11 kcal/mol is smaller than that with the zero-point energy correction. As a result, the classical (1 bead) calculation overestimates the rate, for instance, by a factor of nearly two at 200 K.

As discussed above, the lattice effects manifest themselves primarily in the free energy profile and therefore equally affect the centroid density QTST and RPMD rate coefficients. Table 1 shows that the nickel lattice motion diminishes the rate of hopping when $T \leq 80$ K but enhances it at higher temperatures. The most significant effect is observed at the lowest temperature (T = 30 K), where the lattice motion diminishes the rate by a factor of about two. Note that this is a purely classical phenomenon: the effect of lattice quantization is found to be essentially negligible at all of the temperatures we have considered, in both the QTST and the RPMD calculations.

The change in the effect of the lattice motion as the temperature passes through T_c coincides with the change in the hopping mechanism. Qualitatively, it can be explained by the impact of different local modes of the lattice on the hopping process. Below the crossover temperature, the adsorbate interacts predominantly with the lattice motion in the potential energy well, which can induce a dissipative effect and hinder the tunnelling rate. As the temperature increases, the hopping passes to the overbarrier regime where the adsorbate interacts more with the lattice motion in the barrier region, and this can enhance the hopping by lowering the barrier (phonon-assisted diffusion[62]). The distinction between nickel lattice modes that enhance the hydrogen hopping rate and those that suppress it has been analyzed by Baer et al.[20−22] using the surrogate Hamiltonian method. In this method, the metal degrees of freedom are treated as baths of quantum harmonic oscillators, with the structure of the baths and their interaction with the hydrogen atom being extracted from a classical molecular dynamics simulation. Baer et al. found that the balance between the enhancement and suppression of the hopping caused by the lattice motion is delicate and that the later may overcome the former in the deep-tunnelling regime, which is qualitatively in agreement with the present observations.

IIIC. High-Temperature Diffusion. The picture of diffusion as a succession of uncorrelated site-to-site hops is quite reasonable at low temperatures where the residence time at a given stable site is many vibrational periods. At higher temperatures, the hopping between sites is no longer a rare event, and the possibility of correlated jumps should be taken into account. The only previous theoretical study of this problem that we are aware of is that of Metiu and co-workers,[23−25] who used the flux−flux correlation function formalism within a mixed quantum-classical approach to estimate the contribution of multiple jumps in the temperature range 200−400 K. The diffusion coefficients were calculated using a random walk model incorporating both single and multiple jumps. They found that multiple jumps are important and should not be neglected: the computed diffusion coefficients were 3−4 times larger when the contribution of these jumps was included. They also found that both the amount of transition state recrossing and the contribution of the multiple jumps were very sensitive to the shape of the interaction potential.[23]

In the present study, the assumption of the random walk model also becomes questionable at these temperatures as follows from the long-time behavior of the RPMD transmission coefficients presented on the lower panel of Figure 5. The contribution of multiple jumps to the RPMD diffusion coefficients is, however, not clear. To validate the low-temperature results obtained in Section IIIB using the random walk model and to shed further light on the diffusion process, we have calculated the RPMD diffusion coefficients at 200 K and above using the Green−Kubo and Einstein relations. As discussed in Section IIA, these relations do not make any assumptions about the diffusion mechanism, and they are not tied in any way to the random walk model. Moreover, the

RPMD diffusion coefficients calculated in this way are guaranteed to become exact in the high-temperature (classical) limit.

Figure 6 shows typical plots of the RPMD mean square displacements and velocity autocorrelation functions, obtained for hydrogen diffusion on the rigid and classical lattices at 300 K. The short-time oscillations in these plots arise because the majority of the adsorbed atoms in the canonical ensemble is vibrating around equilibrium surface sites. The oscillations are initially strong but dephase within 1 ps. Eventually the velocity autocorrelation function becomes zero, and the mean square displacement becomes linear in time, as it should for a diffusive process. Diffusion coefficients were calculated from the area under the velocity autocorrelation function and the long time slope of the mean square displacement.

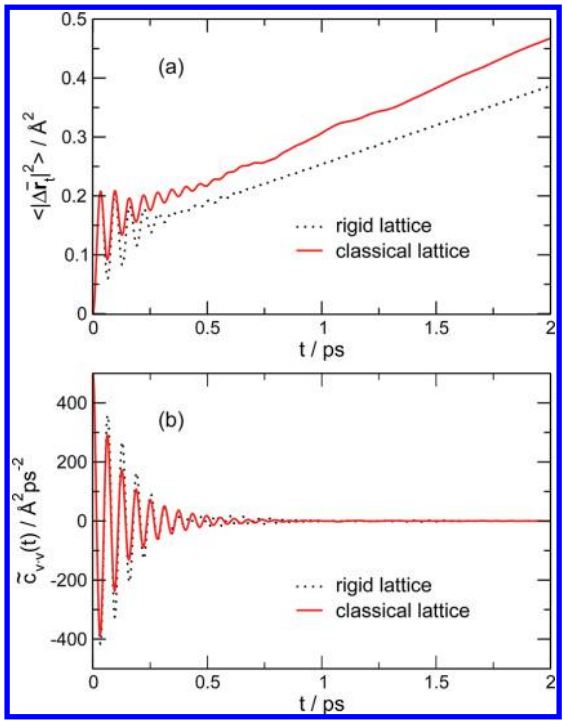

Figure 6. RPMD mean-squared displacement (a) and velocity autocorrelation function (b) versus time for hydrogen on the Ni(100) surface at 300 K. Solid lines correspond to the rigid lattice and dashed lines to the classical lattice.

Table 2 compares the resulting diffusion coefficients with the estimates obtained from the random walk model at temperatures from 200 to 1000 K. The slight difference (up to 5%) between the results obtained from the Einstein and Green–Kubo relations reflects the different way in which the statistical errors in the trajectory calculations enter the averages in eqs 2 and 8. In fact, we were not able to converge the velocity autocorrelation function well enough to obtain a reliable diffusion coefficient from the Green–Kubo relation at 200 K, although the mean squared displacement at this temperature converged satisfactorily.

Table 2 shows that the diffusion coefficients obtained from these simulations are in reasonably good agreement with the random walk model estimates at 200 and 300 K. This is especially true in the case of the classical lattice, for which the difference is within the combined statistical error of around 10% in the various calculations. This suggests that the accuracy of the random walk model is sufficient for comparison with experimental measurements at temperatures below 300 K.

However, the results obtained from this model do begin to deviate from the Green–Kubo and Einstein relation results at higher temperatures. The departure is most noticeable for the classical lattice, where it reaches a factor of nearly two at 1000 K. The fact that the full RPMD diffusion coefficients are *smaller* than those obtained from the random walk model is in direct contrast to the results of Metiu and co-workers described above.[23−25] It suggests that successive site-to-site jumps are correlated and that the RPMD trajectories have a tendency to rebound at high temperatures back to the site from which they originated.[63]

This explanation is supported by Figure 7, which shows histograms of the resonance times in surface sites of the RPMD trajectories on the rigid and classical lattices at 800 K. These histograms were extracted from an ensemble of "diffusive" trajectories that exhibited at least one site-to-site hop within a simulation time of 10 ps. Two histograms are shown in each panel of the figure, one for a quarter of all residence events and the other for residence events that end by rebounding to the site that the trajectory last visited. One sees that at short times, t < 0.25 ps, there is a distinct tendency for trajectories to rebound, making the diffusion coefficient smaller than it would be in a random walk model. Beyond around 0.25 ps, the trajectories have lost all memory of where they came from, and the next jump is equally likely to be in any of the four possible directions. At high temperatures such as 800 K, where the average residence time in a site is on the order of 0.25 ps and the short-time rebounds constitute a significant fraction of all hopping events, the net effect is that the random walk model overestimates the diffusion coefficient. At lower temperatures such as 300 K, there is again a tendency for trajectories to rebound within the first 0.25 ps, but since the average residence time in a site is now considerably longer (on the order of 10 ps)

Table 2. RPMD Diffusion Coefficients for Hydrogen Diffusion on the Ni(100) Surface from the Einstein and Green–Kubo Relations and from the Random Walk Model in the Temperature Interval Between 200 and 1000 K[a]

T (K)	200	300	400	500	600	700	800	900	1000
				Rigid Lattice					
random walk model	1.23 (−7)	4.41 (−6)	2.77 (−5)	8.19 (−5)	1.66 (−4)	2.80 (−4)	4.13 (−4)	5.36 (−4)	6.77 (−4)
Einstein relation	1.11 (−7)	3.31 (−6)	1.93 (−5)	6.03 (−5)	1.21 (−4)	2.26 (−4)	2.99 (−4)	4.22 (−4)	5.63 (−4)
Green–Kubo relation		3.30 (−6)	1.90 (−5)	6.05 (−5)	1.16 (−4)	2.29 (−4)	2.97 (−4)	4.15 (−4)	5.66 (−4)
				Classical Lattice					
random walk model	1.30 (−7)	4.63 (−6)	3.08 (−5)	9.46 (−5)	2.03 (−4)	3.76 (−4)	6.06 (−4)	9.38 (−4)	1.33 (−3)
Einstein relation	1.26 (−7)	4.13 (−6)	2.65 (−5)	7.53 (−5)	1.68 (−4)	2.97 (−4)	4.03 (−4)	5.46 (−4)	7.22 (−4)
Green–Kubo relation		4.26 (−6)	2.61 (−5)	7.55 (−5)	1.65 (−4)	2.98 (−4)	3.97 (−4)	5.38 (−4)	7.10 (−4)

[a]Diffusion coefficients are given in cm^2 s^{-1}, and numbers in parentheses denote powers of ten.

dx.doi.org/10.1021/jp302453z | J. Phys. Chem. C 2012, 116, 11141−11153

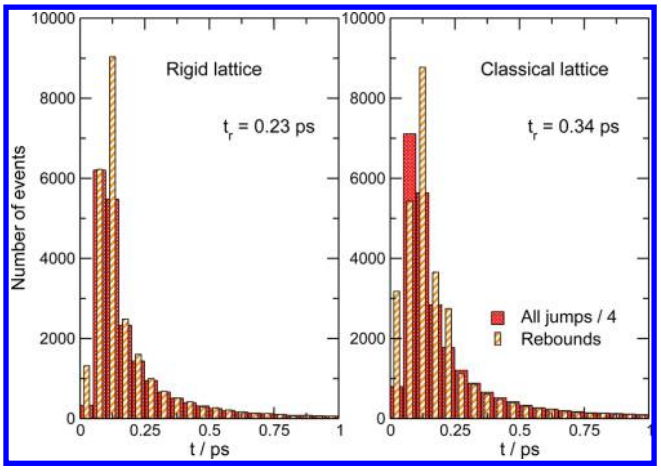

Figure 7. Statistical distribution of site residence times for hydrogen diffusing on the rigid (left) and classical (right) Ni(100) surfaces at 800 K. The total simulation time is 10 ps, and only "diffusive" trajectories are taken into account. Broad yellow bars: total number of residence events in each 0.05 ps histogram bin, divided by four. Narrow red bars: number of residence events for "rebound" trajectories that return to the site from which they came. The average residence time in a surface site t_r is indicated in each panel.

the rebounds constitute a much smaller fraction of all hopping events, and the random walk model only slightly overestimates the diffusion coefficient (see Table 2).

The histograms presented in Figure 7 are very similar for both types of the lattice. However, there are substantial differences in the diffusion processes on the two lattices at all temperatures. For example, Figure 8 shows the centroid paths

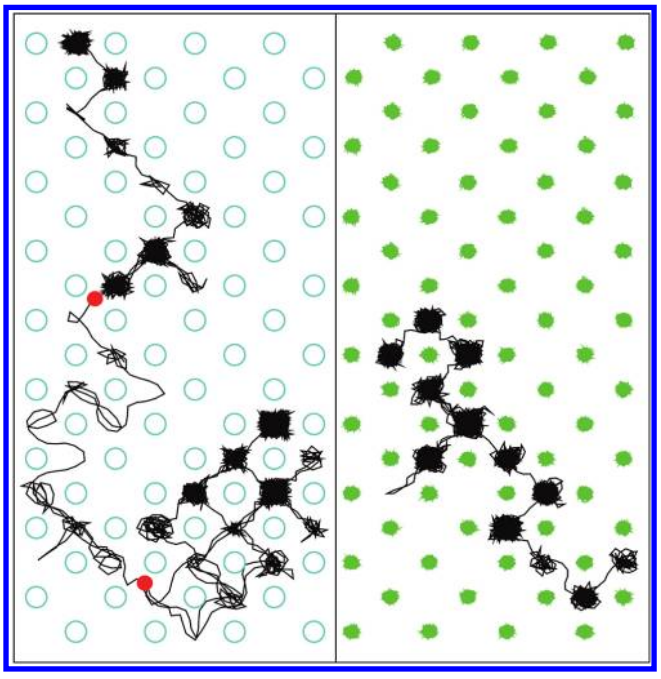

Figure 8. Typical diffusive trajectories of the centroid of the hydrogen atom ring polymer on the Ni(100) surface at 300 K. These trajectories were obtained during a 0.5 ns time interval for the rigid (left panel) and classical (right panel) lattices. For the rigid lattice, the equilibrium positions of the surface atoms are represented by open circles. For the classical lattice, the trajectories of all the surface atoms are presented. The long excursion between the red circles in the left-hand panel only takes around 20 ps.

of two representative hydrogen trajectories at 300 K. For the classical lattice (right panel), the H diffusion is fairly well described within a random walk model. The trajectory is characterized by a series of single jumps separated by periods of vibrations within a given adsorption well. Inspection of the trajectory shows that it also contains a small number of rapid bounce-back jumps which act to decrease the diffusion coefficient. The diffusion across the rigid lattice is not so easily categorized, as shown on the left panel of Figure 8. The hydrogen atom still performs a series of uncorrelated single jumps, and bounce-backs also take place. However, because the atom in this case does not exchange energy with the lattice, it can remain excited long enough to perform a sequence of correlated jumps crossing several unit cells.

One might expect that this tendency for correlated jumps on the rigid surface would result in a higher diffusion coefficient. However, as can be seen from Table 2, the diffusion coefficients obtained from the Einstein and Green−Kubo relations on the rigid lattice are actually lower than those obtained on the classical lattice. The reason for this apparent discrepancy is that in constructing Figures 7 and 8 we have confined our attention to diffusive trajectories that exhibit at least one site-to-site hop within 10 ps. The number of these trajectories is significantly smaller when the lattice atoms are kept fixed. At T = 200 K, only 6% of trajectories perform at least one jump on the rigid surface within 10 ps. The percentage increases with temperature but only reaches 50% at 800 K. On the other hand, most of the trajectories are diffusive on the classical lattice at both temperatures. Clearly, not only can the motion of the surface atoms drain excess kinetic energy from the diffusing hydrogen atom, thus preventing the occurrence of the concerted multiple jumps seen in the left-hand panel of Figure 8, but also it can also activate the hopping by lowering the height of the diffusion barrier through thermal fluctuations. According to Table 2, the balance between these two effects is such that the lattice motion increases the diffusion coefficient by up to 40%.

IIID. Comparison with Earlier Theoretical Work and Experiment. Table 3 summarizes the previous theoretical results that are available for the EAM4 interaction potential.[11] These include the rate coefficients obtained by Wang and Zhao[19] using the centroid density QTST and QI approaches and the rate coefficients obtained by Truong and Truhlar[12] using CVT with the transmission coefficient evaluated within a small-curvature semiclassical adiabatic ground-state approximation (CVT/SCSAG). Note that, to compare them with the present data, we have divided Truong and Truhlar's rate coefficients by the number of equivalent hopping directions, σ = 4.

Comparison with Table 1 shows that our results do not agree very well with those of these previous calculations. Most alarmingly, there is even a marked difference between the present centroid density QTST rates and those obtained by Wang and Zhao.[19] The difference between these two calculations increases with decreasing the temperature and reaches 30% and 60% at 80 K for the rigid and classical lattices, respectively. Moreover, Wang and Zhao observed an altogether different lattice motion effect from that seen in the present calculations: their centroid density QTST rates for the classical lattice in the temperature range 80−200 K are smaller than those for the rigid lattice and decrease even further when the Ni atoms in the vicinity of the adsorbed H atom are treated quantum mechanically.

We have traced this discrepancy between the present QTST results and those of Wang and Zhao to the use of different nickel lattices in the two calculations. In the present study, we

dx.doi.org/10.1021/jp302453z | J. Phys. Chem. C 2012, 116, 11141−11153

Table 3. Theoretical Rate Coefficients for Hydrogen and Deuterium Hopping from One Hollow to Another Adjoining Hollow Site on the Ni(100) Surface Obtained in Previous Calculations[12,19] Using the EAM4 Model of the Interaction Potential[11a]

		T (K)						
method	lattice	40	50	60	80	100	200	300
				Hydrogen Diffusion				
QTST[b]	rigid				1.62 (2)	9.74 (3)	2.26 (8)	
	classical				7.28 (1)	8.03 (3)	1.78 (8)	
	quantum				3.41 (1)	4.04 (3)	1.47 (8)	
QI[b]	rigid	2.25 (0)	2.62 (0)	3.10 (0)	2.05 (2)	1.19 (4)	2.12 (8)	7.32 (9)
	classical				9.85 (1)	8.19 (3)	1.82 (8)	
	quantum	1.40 (−1)	3.65 (−1)	9.73 (−1)	5.31 (1)	5.27 (3)	1.16 (8)	4.98 (9)
CVT/	rigid				3.45 (2)	1.59 (4)	2.41 (8)	8.25 (9)
SCSAG[c]	quantum				5.70 (2)	1.89 (4)	2.48 (8)	8.45 (9)
				Deuterium Diffusion				
CVT/	rigid				4.38 (1)	5.91 (3)	1.81 (8)	6.45 (9)
SCSAG[c]	quantum				4.91 (1)	6.26 (3)	1.85 (8)	6.60 (9)

[a]Rate coefficients are given in s^{-1}, and numbers in parentheses denote powers of ten. [b]Results from ref 19 for a lattice consisting of 162 Ni atoms. [c]Results from ref 12 for a lattice consisting of 817 Ni atoms.

used a four-layer slab comprising 392 Ni atoms with periodic boundary conditions in the lateral directions, as illustrated in Figure 2. The lattice used by Wang and Zhao consisted of 162 atoms in a four-layer slab, with all Ni atoms in the bottom layer and on the sides of the slab held fixed.[19] The comparatively small (30%) differences between our QTST rates and theirs in the case of the rigid lattice arise solely from the smaller lateral dimensions of their lattice, which were less than twice the cutoff distance of the EAM4 potential.[11] The larger and even qualitatively different effects of lattice motion seen in the two calculations arise from Wang and Zhao's use of both a smaller lattice and hard wall boundary conditions. This clearly places more stringent constraints on the lattice motion and leads to higher frequency surface phonon modes than were present in our calculations.

To check this, we have calculated the centroid density QTST rate coefficients at 200 K using the rigid and classical lattices of Wang and Zhao. We obtain 2.15×10^8 and 1.73×10^8 s^{-1}, respectively, in good agreement with their values in Table 3. We have also performed centroid density QTST calculations using their classical lattice at 80 K and obtained a rate of 7.47×10^1 s^{-1}, again consistent with their result.

The QI rates obtained by the same authors[19] exhibit a transition to a nearly temperature-independent regime below 70 K, in good agreement with the present results. However, as in the case of their centroid density QTST calculations, Wang and Zhao found that the effect of (quantized) lattice motion was to diminish the QI rate, giving a suppression of more than an order of magnitude at low temperature (T = 40 K). Because of this lattice motion effect, which we do not see with the larger Ni lattice we have used in the present calculations, their QI rate coefficients are 2−3 times larger than our RPMD rate coefficients for the rigid lattice and 2−4 times smaller than our RPMD rate coefficients when lattice motion is taken into account.[19]

The CVT/SCSAG rate coefficients obtained by Truong and Truhlar[12] also exhibit some inconsistencies with the present results. For the rigid lattice, the CVT/SCSAG method produces larger values of the rate coefficients than the present calculations. The difference becomes more pronounced with decreasing the temperature and reaches a factor of 3 for hydrogen hopping at the lowest temperature available for comparison (T = 80 K). Moreover, allowing for lattice motion is found to increase the CVT/SCSAG rate coefficient at all temperatures above the crossover temperature (67 K) and especially so at 80 K. In the present RPMD calculations, we also find that lattice motion increases the rate of hopping well above the crossover temperature but that the trend reverses, leading to a decreased hopping rate at 80 K and below (see Table 1).

While we do not have a clear explanation for the differing effects of lattice motion on the CVT/SCSAG and RPMD hopping rates, it is perhaps worth noting that the lattice used in the CVT/SCSAG calculations was also different from that used in the present study. Truong and Truhlar used a larger lattice than us (composed of 817 Ni atoms arranged in 9 layers). However, only the 8 Ni atoms closest to the diffusion path were allowed to move (see ref 12 for details), and it is possible that this restricted description of the lattice motion may have had some effect on the computed CVT/SCSAG rate. Indeed, a more recent study by Wonchoba and Truhlar[64] of hydrogen diffusion on the Cu(100) surface has shown that the CVT/SCSAG rate can be very sensitive to the number of mobile lattice atoms. Another possible explanation for the different effects of lattice motion in the RPMD and CVT/SCSAG calculations is that the geometric approximation to the reaction path in the SCSAG transmission coefficient can have a strong influence on the diffusion on a nonrigid surface.[62,64] Overall, the comparison with previous calculations reveals that the rate is sensitive not only to the choice of the theoretical method but also to the structural model that is used to compute it.

At this point it is useful to compare the present theoretical results with the available experimental data.[2−4,6] First of all, it should be noted that the experiments were performed at nonzero coverages, and this prevents a rigorous quantitative comparison to calculations performed with a single adatom. However, the coverage dependence of the measured diffusion coefficients was found to be weak,[4,6] indicating that the theoretical extrapolation to zero coverage should be valid for a semiquantitative comparison with experiment.

Figure 9 presents an Arrhenius plot of the measured diffusion coefficients along with the QI[19] and RPMD diffusion coefficients obtained using the random walk model. Theory and experiment are seen to be in reasonable agreement at high temperatures (T > 250 K), indicating that the height of the diffusion barrier on the EAM4 potential is approximately

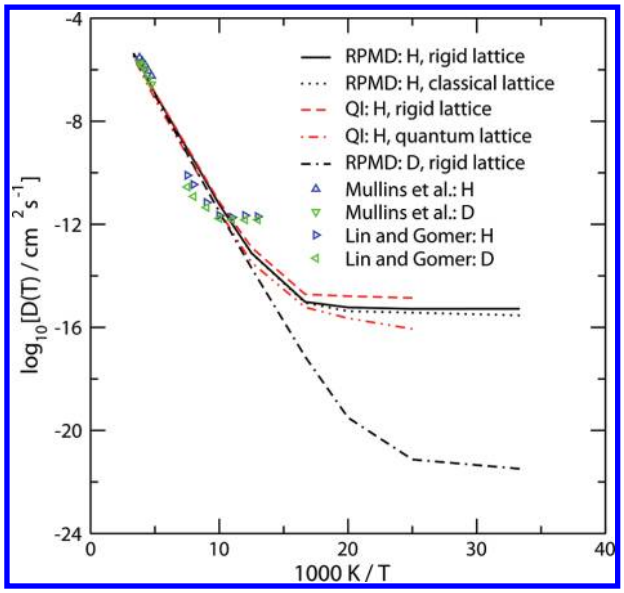

Figure 9. Arrhenius plots of the diffusion coefficients of H and D in the temperature range 30−300 K. The present RPMD results within the random walk model are compared with the QI results of Wang and Zhao,[19] the high-temperature experimental results of Mullins et al.,[3] and the low-temperature experimental results of Lin and Gomer.[4] The experimental results of George et al.[2] are similar to those of Mullins et al.,[3] and the results of Lee et al.[6] are similar to those of Lin and Gomer.[4]

correct. However, the agreement is far worse at temperatures in the tunnelling regime (T < 150 K), indicating that the width (or curvature) of the diffusion barrier is likely to be wrong. For hydrogen, the experimental results of Lin and Gomer[4] show a clear transition to activationless diffusion at around 100 K, whereas this does not occur in the theoretical calculations until around 70 K (consistent with the parabolic barrier transition temperature on the EAM4 potential of 67 K, assuming that most of the tunnelling below this temperature is from the ground quantum state of the H atom in its adsorption site and therefore insensitive to any further reduction in the temperature). The comparatively minor differences between the QI and RPMD results are insignificant compared with the disagreement between theory and experiment, as are the differences between the various flavours of RPMD calculation (rigid lattice, classical lattice, quantum lattice). All of the theoretical calculations that have been performed using the EAM4 potential at these low temperatures predict a transition to activationless H diffusion at around 70 K.

To make matters worse, there is a *qualitative* disagreement between the experimental results of Lin and Gomer[4] and the present RPMD calculations with regard to the H/D kinetic isotope effect in the deep tunnelling regime. The calculations and experiments agree that there is very little difference between the rates of H and D diffusion and that the activation energies of both processes are the same before tunnelling sets in. However, whereas the onset of deuterium tunnelling in the calculations is shifted down to 50 K, consistent with the lower parabolic barrier frequency for D than for H, the experiment finds the transition temperatures for the two isotopes to be the same.

It is possible that this discrepancy between the theoretical results and experiment may be due to the deficiencies of the EAM4 interaction potential[11] used in the calculations. A similar transition temperature has been calculated for subsequent version of the EAM interaction potential (EAM5).[13] The main shortcomings of the EAM potentials arise from the fact that they are fit to experimentally determined properties which are most sensitive to equilibrium configurations.[7,8] The shape of the potential along the diffusion path will be more important when dealing with diffusion in the tunnelling regime.[65]

On the other hand, it is hard to see how a calculation using *any* potential could give the same tunnelling transition temperature for H and D. The H and D transition temperatures observed in the present calculations (70 and 50 K) are very close to the parabolic barrier estimates (67 and 48 K), which differ by a simple mass factor of around $1/\sqrt{2}$. In a scanning tunnelling microscopy study of the diffusion of isolated H and D atoms on a Cu(100) surface, Lauhon and Ho[66] have observed a distinct transition from thermally activated diffusion to quantum tunnelling of the H atom at 60 K but no evidence of a transition to tunnelling for the D atom at temperatures down to 50 K. This is clearly consistent with the transition temperature being around $1/\sqrt{2}$ times smaller for D than for H, at 42.5 K.

It is therefore possible that the qualitative discrepancy between the calculations and the low-temperature experimental data in Figure 9 is due to an experimental problem. The experiment of Lin and Gomer is subject to the effects of steps and defects on the surface as well as adsorbate−adsorbate interactions, none of which have been taken into account in the present calculations. There are also known difficulties in establishing absolute values for the diffusion rate from field emission microscopy data.[67] The locations of the experimental transition temperatures clearly require refinement, as suggested by Cao et al.[68] To draw any further conclusion, it seems important both to refine the experimental data and to construct a more accurate model of the potential energy surface from first-principles calculations.

IV. SUMMARY

In this paper, we have presented a detailed ring polymer molecular dynamics study of the diffusion of hydrogen on Ni(100), using the EAM4 interaction potential.[11] We have paid particular attention to the effects of lattice motion, transition state recrossing, and multiple hops, all of which can be assessed within a unified theoretical framework using RPMD.

First, we studied the low-temperature regime where the diffusion process can be represented as a sequence of uncorrelated single site-to-site hops. The rate of these hops was calculated using the Bennett−Chandler method[48,49] as a product of a static (centroid density QTST rate) and a dynamic (transmission coefficient) factor. We found a crossover at around 70 K from thermally activated diffusion to almost temperature-independent quantum diffusion, in agreement with earlier quantum instanton calculations.[19] The rate coefficient is well approximated by centroid density QTST above the crossover temperature, but below crossover the recrossing of the centroid dividing surface becomes more significant. The lattice motions mainly influence the static contribution to the rate rather than the dynamic contribution. We have found that the lattice motion slightly increases the rate above and slightly decreases the rate below the crossover temperature. Qualitatively, this can be explained by the different impact of the local modes of the lattice near the potential well and in the barrier region on the hopping mechanism. We have also found that quantizing the motion of the metal atoms has a negligible effect, even at very low temperatures. These last two observations are at variance with previous theoretical

results[12,19] obtained using the same interaction potential. We have argued that this is primarily due to the different lattice models employed in the various calculations.

Second, we studied the high-temperature regime. The diffusion coefficients were computed using the Einstein[43,44] and Green−Kubo[42−44] relations. Comparison of these results with those generated by the random walk model allowed us to examine the role of correlated dynamical events in the diffusion. No significant difference between the diffusion coefficients obtained by the two approaches was found at temperatures up to 300 K. The neglect of correlated and multiple jump contributions is therefore valid at the temperatures of the experimental measurements.[2,3] At higher temperatures, however, we found a noticeable contribution of correlated rebound events in our Einstein and Green−Kubo calculations leading to a decrease in the diffusion coefficient compared to the random walk estimate.

Important discrepancies between experiment and theory are still unresolved. The present calculations find that the crossover from activated diffusion to quantum tunnelling occurs at a significantly lower temperature than in the experiment of Lin and Gomer,[4] and they do not reproduce the anomalously small H/D isotope effect that is seen experimentally. From a theoretical point of view, the next natural step would be to repeat the present study using more accurate potential energy function from a first-principles calculation.

AUTHOR INFORMATION

Corresponding Author

*E-mail: yury.suleymanov@gmail.com.

Present Address

[†]Department of Chemical Engineering, Massachusetts Institute of Technology, Cambridge, Massachusetts 02139.

Notes

The authors declare no competing financial interest.

ACKNOWLEDGMENTS

I would like to thank Thomas Markland for helping me to get started with this project and David Manolopoulos for extensive comments on an early draft of this manuscript. An allocation of computer time on the Western Canada Research Grid (WestGrid) is gratefully acknowledged. This work was supported by a Newton International Fellowship from the Royal Society.

REFERENCES

(1) Samorjai, G. A.; Li, Y. *Introduction to surface chemistry and catalysis*; John Wiley & Sons: NJ, 2010.

(2) George, S. M.; Desantolo, A. M.; Hall, R. B. *Surf. Sci.* **1985**, *159*, L425−L432.

(3) Mullins, D. R.; Roop, B.; Costello, S. A.; White, J. M. *Surf. Sci.* **1987**, *186*, 67−74.

(4) Lin, T. S.; Gomer, R. *Surf. Sci.* **1991**, *255*, 41−60.

(5) Zhu, X. D.; Lee, A.; Wong, A.; Linke, U. *Phys. Rev. Lett.* **1992**, *68*, 1862−1865.

(6) Lee, A.; Zhu, X. D.; Deng, L. *Phys. Rev. B* **1992**, *46*, 15472−15476.

(7) Foiles, S. M.; Baskes, M. I.; Daw, M. S. *Phys. Rev. B* **1986**, *33*, 7983−7991.

(8) Daw, M. S.; Baskes, M. I. *Phys. Rev. B* **1984**, *29*, 6443−6453.

(9) Rice, B. M.; Garrett, B. C.; Koszykowski, M. L.; Foiles, S. M.; Saw, M. S. *J. Chem. Phys.* **1990**, *92*, 775−791.

(10) Truong, T. N.; Truhlar, D. G.; Garrett, B. C. *J. Phys. Chem.* **1989**, *93*, 8227−8239.

(11) Truong, T. N.; Truhlar, D. G. *J. Phys. Chem.* **1990**, *94*, 8262−8279.

(12) Truong, T. N.; Truhlar, D. G. *J. Chem. Phys.* **1990**, *93*, 2125−2138.

(13) Wonchoba, S. E.; Hu, W.-P.; Truhlar, D. G. *Phys. Rev. B* **1995**, *51*, 9985−10002.

(14) Wonchoba, S. E.; Truhlar, D. G. *Phys. Rev. B* **1996**, *53*, 11222−11241.

(15) Mattsson, T. R.; Engberg, U.; Wahnström, G. *Phys. Rev. Lett.* **1993**, *71*, 2615−2618.

(16) Mattsson, T. R.; Wahnström, G. *Phys. Rev. B* **1995**, *51*, 1885−1896.

(17) Mattsson, T. R.; Wahnström, G. *Phys. Rev. B* **1997**, *56*, 14944−14947.

(18) Mattsson, T. R.; Wahnström, G.; Bengtsson, L.; Hammer, B. *Phys. Rev. B* **1997**, *56*, 2258−2266.

(19) Wang, W.; Zhao, Yi. *J. Chem. Phys.* **2009**, *130*, 114708.

(20) Baer, R.; Zeiri, Y.; Kosloff, R. *Surf. Sci.* **1998**, *411*, L783−L788.

(21) Baer, R.; Kosloff, R. *J. Chem. Phys.* **1997**, *106*, 8862−8875.

(22) Baer, R.; Zeiri, Y.; Kosloff, R. *Phys. Rev. B* **1997**, *55*, 10952−10974.

(23) Zhang, Z.; Metiu, H. *J. Chem. Phys.* **1990**, *93*, 2087−2098.

(24) Zhang, Z.; Haug, K.; Metiu, H. *J. Chem. Phys.* **1990**, *93*, 3614−3634.

(25) Haug, K.; Metiu, H. *J. Chem. Phys.* **1991**, *94*, 3251−3267.

(26) Craig, I. R.; Manolopoulos, D. E. *J. Chem. Phys.* **2004**, *121*, 3368−3373.

(27) Braams, B. J.; Manolopoulos, D. E. *J. Chem. Phys.* **2006**, *125*, 124105.

(28) Miller, T. F.; Manolopoulos, D. E. *J. Chem. Phys.* **2005**, *122*, 184503.

(29) Craig, I. R.; Manolopoulos, D. E. *Chem. Phys.* **2006**, *322*, 236−246.

(30) Miller, T. F.; Manolopoulos, D. E. *J. Chem. Phys.* **2005**, *123*, 154504.

(31) Miller, T. F. *J. Chem. Phys.* **2008**, *129*, 194502.

(32) Markland, T. E.; Habershon, S.; Manolopoulos, D. E. *J. Chem. Phys.* **2008**, *128*, 194506.

(33) Markland, T. E.; Morrone, J. A.; Berne, B. J.; Miyazaki, K.; Rabani, E.; Reichman, D. R. *Nat. Phys.* **2011**, *7*, 134−137.

(34) Craig, I. R.; Manolopoulos, D. E. *J. Chem. Phys.* **2005**, *122*, 084106.

(35) Craig, I. R.; Manolopoulos, D. E. *J. Chem. Phys.* **2005**, *123*, 034102.

(36) Collepardo-Guevara, R.; Craig, I. R.; Manolopoulos, D. E. *J. Chem. Phys.* **2008**, *128*, 144502.

(37) Collepardo-Guevara, R.; Suleimanov, Yu. V.; Manolopoulos, D. E. *J. Chem. Phys.* **2009**, *130*, 174713; **2010**, *133*, 049902.

(38) Boekelheide, N.; Salomón-Ferrer, R.; Miller, T. F. *Proc. Natl. Acad. U.S.A.* **2011**, *108*, 16159−16163.

(39) Menzeleev, A. R.; Ananth, N.; Miller, T. F. *J. Chem. Phys.* **2011**, *135*, 074106.

(40) Suleimanov, Yu. V.; Collepardo-Guevara, R.; Manolopoulos, D. E. *J. Chem. Phys.* **2011**, *134*, 044131.

(41) Perez de Tudela, R.; Aoiz, F. J.; Suleimanov, Yu. V.; Manolopoulos, D. E. *J. Phys. Chem. Lett.* **2012**, *3*, 493−497.

(42) Green, M. S. *J. Chem. Phys.* **1952**, *20*, 1281−1295; **1954**, *22*, 398−413. Kubo, R.; Yokota, M.; Nakajima, S. *J. Phys. Soc. Jpn.* **1957**, *12*, 1203. McQuarrie, D. A. *Statistical Mechanics*; Harper and Row: New York, 1976.

(43) Allen, M. P.; Tildesley, D. J. *Computer Simulation of Liquids*; Oxford University Press: Oxford, 1987.

(44) Doll, J. D.; Voter, A. F. *Annu. Rev. Phys. Chem.* **1987**, *38*, 413−431.

(45) Chandler, D.; Wolynes, P. G. *J. Chem. Phys.* **1981**, *74*, 4078−4095.

(46) Feynman, R. P.; Hibbs, A. R. *Quantum Mechanics and Path Integrals*; McGraw-Hill: New York, 1965.

(47) Chandrasekhar, S. *Rev. Mod. Phys.* **1943**, *15*, 1−89.

(48) Bennett, C. H. In *Algorithms for Chemical Computations*, ACS Symposium Series No. 46; Christofferson, R. E., Ed.; American Chemical Society: Washington DC, 1977; p 63.
(49) Chandler, D. *J. Chem. Phys.* **1978**, *68*, 2959−2970.
(50) Gillan, M. J. *Phys. Rev. Lett.* **1987**, *58*, 563−566; *J. Phys. C* **1987**, *20*, 3621−3641.
(51) Voth, G. A.; Chandler, D.; Miller, W. H. *J. Chem. Phys.* **1989**, *91*, 7749−7760.
(52) Wang, W.; Zhao, Yi. *J. Chem. Phys.* **2010**, *132*, 064502.
(53) Kästner, J.; Thiel, W. *J. Chem. Phys.* **2005**, *123*, 144104.
(54) Kästner, J.; Thiel, W. *J. Chem. Phys.* **2006**, *124*, 234106.
(55) Kästner, J. *J. Chem. Phys.* **2009**, *131*, 034109.
(56) Andersen, H. C. *J. Chem. Phys.* **1980**, *72*, 2384−2393.
(57) Andersen, H. C. *J. Comput. Phys.* **1983**, *52*, 24−34.
(58) Richardson, J. O.; Althorpe, S. C. *J. Chem. Phys.* **2009**, *131*, 214106.
(59) Makarov, D. E.; Topaler, M. *Phys. Rev. E* **1995**, *52*, 178−188.
(60) Struchebrukov, A. A. *J. Chem. Phys.* **1991**, *95*, 4258−4276.
(61) Mills, G.; Schenter, G. K.; Markov, D. E.; Jónsson, H. *Chem. Phys. Lett.* **1007**, *278*, 91−96.
(62) Truong, T. N.; Truhlar, D. G. *J. Phys. Chem.* **1987**, *91*, 6229−6237.
(63) Cohen, J. M.; Voter, A. F. *J. Chem. Phys.* **1989**, *91*, 5082−5086.
(64) Wonchoba, S. E.; Truhlar, D. G. *J. Chem. Phys.* **1993**, *99*, 9637−9651.
(65) Bhatia, B.; Sholl, D. S. *J. Chem. Phys.* **2005**, *122*, 204707.
(66) Lauhon, L. J.; Ho, W. *Phys. Rev. Lett.* **2000**, *85*, 4566−4569.
(67) Daniels, E. A.; Gomer, R. *Surf. Sci.* **1995**, *336*, 245−261.
(68) Cao, G. X.; Nabighian, E.; Zhu, X. D. *Phys. Rev. Lett.* **1997**, *79*, 3696−3699.